Silicon (2023) 15:2185–2197
https://doi.org/10.1007/s12633-022-02162-z

ORIGINAL PAPER

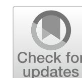

Investigation of DS Furnace Heat Exchange Block Thickness for the Improvement mc-Si Ingot Quality

Anbu Gopalakrishnan[1] · Thiyagarajan Madhu[1,2] · Aravindan Gurusamy[1] · Srinivasan Manickam[1] · Ramasamy Perumalsamy[1]

Received: 22 April 2022 / Accepted: 5 October 2022 / Published online: 18 October 2022
© Springer Nature B.V. 2022

Abstract

Numerical investigation was performed for analyzing the distribution of von Mises stress in the growing multi-crystalline silicon ingot during the directional solidification process. In order to minimize the generation of the dislocation density, it is important to grow the mc-Si ingot with lower von Mises stress by maintaining 600 mbr pressure and Ar gas is inlet 20 LPM throughout the growth process. The important features for the generation of von Mises stress in the growing mc-Si ingot is axial and radial temperature gradient. The axial and radial temperature distributions play vital role for the generation of von Mises stress. By varying the thickness of the heat exchanger block the axial temperature distribution got altered. Directional Solidification furnace with various thickness of heat exchanger block (50 mm—250 mm) has been simulated and their response to solidification process has been analyzed. The distribution of axial and radial temperature, maximum principal stress and shear stress studies have been carried out for analyzing the distribution of von Mises stress in the mc-Si ingot. The growth rate of the mc-Si ingot has been altered by varying the thickness of the heat exchanger block. Since we maintained the growth rate within the optimal range, the optimal stress distribution has been observed for all the cases due to the lower growth rate. The recommended thickness of the heat exchanger block thickness is 250 mm.

Keywords Silicon solar cell · Computer simulation · Directional solidification · Thermal stress · Heat exchanger block thickness

1 Introduction

The market of Directional Solidification (DS) process grown multi-crystalline Silicon (mc-Si) has increased steadily in PV industry due to the higher throughput. The cost of silicon wafers can be decreased and production efficiency can be improved by increasing the size of the silicon ingot. However, controlling the thermal field when the hot zone is larger in order to produce high-quality ingots is one of the difficulties in producing large-size silicon ingots. With changes to design or growth parameters high-quality ingots can be made. In order to acquire the temperature and flow field, the distribution of thermal stress and the form of melt crystal interface shape of silicon ingot during the solidification process by numerical simulation has proven to be an efficient method [1, 2]. Several investigations have been done to enhance the thermal field and thermal stress. Investigation of the impact of changing of geometry on thermal distribution and flow field is done using transient simulations [3, 4]. The effect of heat exchanger block (HEB) in the distribution of temperature and VMS in the grown multi-crystalline silicon ingot is studied by Nagarajan et al. [5] and the results reveal the additional insulation block in the hot zone increases the crystal quality with consuming less power. Comparative study of three different size DS furnace 7 kg, 40 kg and 330 kg grown mc-Si ingots investigated [6]. Su et al. have investigated bottom grille thermal filed, flow filed, c/m interface shape and growth rate [7]. By adding an additional insulation on the hot zone of the DS furnace, Aravindan et al. enhance the mc-Si ingot quality [8]. The presence of grain boundaries in the mc-Si ingot limits the conversion efficiency of the solar cell. During the growth process, many dislocations were generated from the higher

✉ Anbu Gopalakrishnan
anvini777@gmail.com

[1] Department of Physics, Sri Sivasuramaniya Nadar College of Engineering, Chennai 603110, India

[2] Division of Physics, School of Advance Science, Vellore Institute of technology, Chennai 600127, India

stress places [9]. The segregation of metallic impurities on the grain boundaries limits the lifetime of the minority carriers. At the time of the growth process, it is essential to grow the multi-crystalline silicon ingot with the lower thermal stress which is responsible for dislocation generation. Dislocations produce the plastic deformation which can cause the stress relaxation during the growth stage and the arising of high residual stress on the cooling stage which may result in ingot cracking. Growing mc-Si ingot with larger grain size by preserving the seed assisted crystal at the bottom of the crucible is one technique to improve the quality of the ingot, whereas growing mc-Si ingot with optimal grain boundaries is another technique to obtain electrically inactive lower energy grain boundaries. Anis Jouinil et al. have investigated the growth of dendritic crystals for obtaining the lower energy grain boundaries [10]. Kakimoto et al. studied the single seeded casting technique from which they have grown mono-crystalline like silicon [11, 12]. Bing et al., have compared solidification process by using single heat gate and multiple heat gate configuration [13]. Chen et al. have studied the VMS for different solidification times (6 h, 10 h, and 15 h) and they observed that the shorter solidification time leads to higher VMS whereas higher solidification time leads to lower VMS [14]. Zhiyoung wu et al. have studied the solidification process with the partition block in which they have moved the partition block with different velocities. At particular velocity of partition block, they have observed the minimum VMS [15]. Wang et al., have proposed a single heater on DS furnace in which they have studied the VMS with different gas flow velocity. (0.05 m/s, 0.22 m/s, 0.3 m/s, 0.4 m/s and 0.6 m/s). Minimum VMS of 13.66 MPa has been found for flow velocity 0.05 m/s [16]. Naigen Zhou et al., have investigated VMS by decreasing side insulation thickness and by moving the heater up side [17]. Aravindan et al. have numerically investigated thermal stress for different annealing time. At particular annealing time (5 h) they have observed the minimum VMS [18]. Xinming haung et al. studied the thermal field distribution in the hot zone by designing the DS furnace with insulated crucible susceptor by which they preserved the seed crystals during the mc-Si ingot. [19]. Zhiyong Wu et al. have reported the distribution of temperature and VMS in the mc-Si ingot through introducing movable heat exchanger block (HEB) in the DS furnace. [5]. Lijun Liu et al. have reported the distribution of temperature and VMS by introducing the insulation partition in the DS furnace to grow the good quality multi-crystalline silicon ingot. [20]. Shi Qiu et al. [21] reported the influence of vacuum in a multicrystalline silicon. Current work, investigates the influence of HEB thickness on the growth of multi-crystalline silicon ingot. The growth rate, axial-radial temperature gradient, maximum principal stress and shear stress, and VMS have been analysed by varying the thickness of the heat exchanger block. The importance of choosing the optimal thickness of the heat exchanger block to get the good quality as well as to grow the ingot with minimum power consumption has been discussed.

2 Model Description

DS process is a simpler process technique compared to CZ process to grow silicon ingots for PV application. Comparing to CZ technique DS technique is a low cost, mass production, low LID effect, and perfect square shape crystal. Directional solidification is the cost-effective technique for the manufacture of mc-Si ingot for PV application. Heat is extracted from the bottom of the crucible and crystal growth is started from the bottom of the crucible. The entire growth is controlled in a single direction which is called directional solidification process [22]. From the initial melting to the final growth stage of ingot, a protective argon atmosphere was maintained by supplying 20 L per minute of argon into the furnace chamber with 600 mbr pressure. The numerical simulation becomes a prevailing technique for improving quality of large size crystal with less cost and time compared to the experimental crystal growth process. Modeling and simulation of crystal growth process has been employed to investigate the preliminary physical phenomena of the growth process and to recommend modifications of design and processes in the existing systems [23]. Simulation has been done for various thickness of HEB. The system comprises quartz crucible, graphite susceptor, heat exchanger block, top heater, side heater, bottom insulation, top insulation, side insulation, melt, crystal and argon gas. The cell number of quartz crucible, graphite susceptor, heat exchanger block, top heater, side heater, bottom insulation, top insulation, side insulation melt, crystal and argon gas is 832, 280, 1072, 90, 90, 449, 1316, 1431, 3071, 2048 and 2338. The cells of quartz crucible, graphite susceptor, heat exchanger block, top heater, side heater, bottom insulation, top insulation, side insulation, melt, crystal and argon gas are of size 0.0298m^3, 0.0286 m^3, 0.0073 m^3, 0.0024 m^3, 0.0013 m^3, 0.0548 m^3, 0.1269 m^3, 0.6442 m^3, 0.1359 m^3, 0.0127 m^3 and 0.1082 m^3. Schematic view of DS system is shown in Fig. 1. Material properties are listed in Table 1. The silicon feed materials are loaded into quartz crucible and fully melted under argon gas atmosphere. In the upward direction, the side insulation is raised at the time of solidification process. The appropriate temperature gradient in the silicon material is kept during the DS process by changing the HEB thickness. Firstly, nucleation initiates at the bottom of the crucible and initiates multi-crystalline silicon ingot grown in bottom to top direction by the heat flux [24]. The CGSim (Crystal Growth simulator) was employed for the computational calculation. Furnace was presumed as 2-D axisymmetric in accordance with real structure of DS system

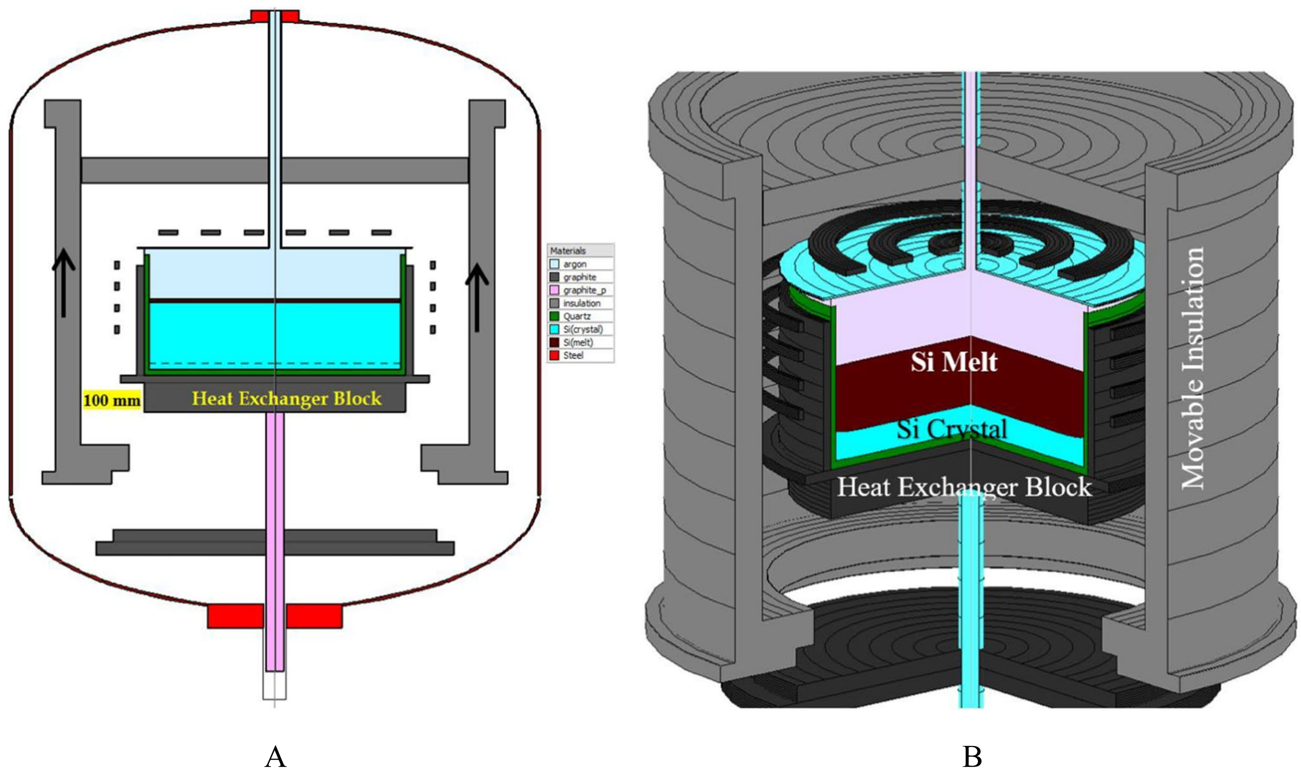

Fig. 1 Schematic diagram of DS furnace. A and B is 2D and 3 D view of DS system

in the numerical model, and separated into sub-regions for simulation. The temperature was set as 1685 K during the crystallization at interface [25]. Then, thermal field inside the DS furnace during the growth process of multicrystalline silicon ingot was calculated. Real quadrangle geometry requires 3-D simulations. What we did is 2-D axisymmetric simulations which, in turn, requires much less computational mesh cells and, consequently, less computational resources, both time and memory. The reference temperature of 1685 K is maintained at the melt/crystal interface within the argon filled DS system [26].

3 Mathematical Model

The governing equations of the momentum balance in an axi-symmetric model.

$$\frac{1}{r}\frac{\partial}{\partial r}\left(r\sigma_{rr}\right) + \frac{\partial}{\partial z}\left(r\sigma_{rz}\right) - \frac{\sigma_{\varphi\varphi}}{r} = 0 \tag{1}$$

$$\frac{1}{r}\frac{\partial}{\partial r}\left(r\sigma_{rz}\right) + \frac{\partial}{\partial z}\left(r\sigma_{zz}\right) = 0 \tag{2}$$

where, normal stress in axial, radial and azimuthal direction, and shear stress is denoted as σ_{zz}, σ_{rr}, $\sigma_{\varphi\varphi}$ and σ_{rz}, respectively.

Simulation was carried out for the cylindrical crucible and it is converted to the square crucible by the calculation. Conversion calculation details are as follows:

$$\mathrm{R}_{\mathrm{cr}} = \frac{2}{\pi^{0.5}} H_{cr}$$

$$H_{cr} = \frac{R_{cr}\pi^{0.5}}{2}$$

where R_{cr} is radius (in cylinder form) of crucible and H_{cr} is half length (in square form) of crucible diameter.

The governing equations of mass transport, heat transport and species transport are as follows:

$$\frac{\partial \rho}{\partial t} + \nabla.\left(\rho\vec{u}\right) = 0$$

$$\frac{\partial(\rho C_p T)}{\partial t} + \nabla.\left(\rho C_p \vec{u} T\right) = \nabla.\left(\lambda_{eff}\nabla T\right) - \nabla.\overrightarrow{q_{rad}} + S_T$$

$$\frac{\partial(\rho\varphi_i)}{\partial t} + \nabla.\left(\rho\vec{u}\varphi_i\right) = \nabla.\left(D_{\varphi_i eff}\nabla\varphi_i\right) + S_{\varphi_i}$$

where ρ is density, $\vec{u}$ is velocity, C_p is specific heat, T is temperature, $\lambda_{eff} = \lambda + \frac{C_p\mu_t}{Pr_t}$ is the effective thermal conduc-

Table 1 Properties of DS furnace components

Material	Properties	Values	Units
Argon	Heat conductivity	0.01	$W\ m^{-1}\ K^{-1}$
	Heat capacity	521	$J\ kg^{-1}\ K^{-1}$
	Dynamic Viscosity	$P(T) = 8.466 \times 10^{-6} + 5.365 \times 10^{-8}\ T - 8.682 \times 10^{-12} T^2$	Pa S
Graphite	Heat conductivity	$P(T) = 146.8885–0.17687\ T + 0.000127T^2 - 4.6899 \times 10^{-008} T^3 + 6.665 \times 10^{-012} T^4$	$W\ m^{-1}\ K^{-1}$
	Emissivity	0.8	
	Density	1950	$kg\ m^{-3}$
	Heat capacity	710	$J\ kg^{-1}\ K^{-1}$
Insulation	Heat conductivity	0.5	$W\ m^{-1}\ K^{-1}$
	Emissivity	0.8	
	Density	500	$kg\ m^{-3}$
	Heat capacity	100	$J\ kg^{-1}\ K^{-1}$
Quartz	Heat conductivity	4	$W\ m^{-1}\ K^{-1}$
	Emissivity	0.85	
	Heat capacity	1232	$J\ kg^{-1}\ K^{-1}$
	Density	2650	$kg\ m^{-3}$
Steel	Heat conductivity	15	$W\ m^{-1}\ K^{-1}$
	Emissivity	0.45	
	Heat capacity	1000	$J\ kg^{-1}\ K^{-1}$
	Density	7800	$kg\ m^{-3}$
Si Melt	Heat conductivity	66.5	$W\ m^{-1}\ K^{-1}$
	Emissivity	0.3	
	Density	$P(T) = 3194–0.3701\ T$	$kg\ m^{-3}$
	Melting Temperature	1685	K
	Surface tension	0.7835	$N\ m^{-1}$
	Dynamic viscosity	0.0008	Pa S
	Heat capacity	915	$J\ kg^{-1}\ K^{-1}$
	Wetting angle	11	Deg
	Latent Heat	1,800,000	$J\ kg^{-1}$
Si crystal	Heat conductivity	$P(T) = 110.6122042–0.1507227384\ T + 0.0001093579825T^2 - 4.009416795 \times 10^{-008} T^3 + 5.66839358 \times 10^{-012} T^4$	$W\ m^{-1}\ K^{-1}$
	Emissivity	$P(T) = 0.9016–0.00026208\ T$	
	Density	2530	$kg\ m^{-3}$
	Latent Heat	1,800,000	$J\ kg^{-1}$
	Heat capacity	1000	$J\ kg^{-1}\ K^{-1}$

tivity, Pr_t=0.9 is the turbulent Prandtl number, $\overrightarrow{q_{rad}}(r) = \int_0^\infty \oint_{4\pi} \Omega I_\lambda(r,\Omega) d\Omega d\lambda$ is the vector radiative heat flux, $I_\lambda(r,\Omega)$ is the intensity of the radiation at the point r, λ is the wavelength of the radiation, $D_{\varphi_i eff}$ is the effective dynamic diffusivity, $S_{\varphi_i} = S^u_{\varphi_i} + \phi_i S^P_{\varphi_i}$ stands for the ith species source. Fluid flow is incompressible. The melt flow was considered as laminar by using the Navier–Stokes equations.

Finite Volume Method (FVM) is used to study the solid material confined by the surface (S) and integral formulation is essential in a control volume (V), it is derived from Eqs. (1) and (2), written as

$$\int_S (\sigma_{rr} n_r + \sigma_{rz} n_z) dS - \int_V \frac{\sigma_{\varphi\varphi}}{r} dV = 0, \tag{3}$$

$$\int_S (\sigma_{rz} n_r + \sigma_{zz} n_z) dS = 0, \tag{4}$$

where, normal unit vector surface of the radial components and axial components are denoted as n_r and n_z, respectively.

The stress–strain relation of an anisotropic thermoelastic solid body can be given by

$$\begin{pmatrix} \sigma_{rr} \\ \sigma_{\varphi\varphi} \\ \sigma_{xx} \\ \sigma_{rz} \end{pmatrix} = \begin{pmatrix} c_{11} & c_{12} & c_{13} & 0 \\ c_{21} & c_{22} & c_{23} & 0 \\ c_{31} & c_{23} & c_{33} & 0 \\ 0 & 0 & 0 & c_{44} \end{pmatrix} \begin{pmatrix} \epsilon_{rr} - \beta_{11}\Delta T \\ \epsilon_{\varphi\varphi} - \beta_{22}\Delta T \\ \epsilon_{zz} - \beta_{33}\Delta T \\ \epsilon_{rz} \end{pmatrix} \tag{5}$$

where ΔT = Temperature- Reference temperature (T-T_{ref}). β_{ij} is the thermal expansion coefficient and crystal elastic coefficient C_{ij}. Three independent elastic coefficients for cubic crystal structure Cij, i.e., C_{11} C_{12} C_{44}. All other coefficients of the silicon can be written as, $C_{22} = C_{33} = C_{11} = 165.77$ Gpa, $C_{23} = C_{13} = C_{12} = 63.93$ Gpa, $C_{44} = 79.92$ Gpa. Also, $\beta_{11} = \beta_{22} = \beta_{33} = 4.5\times 10^{-6}\ K^{-1}$ [5]. The strains ϵ_{ij} can be calculated by

$$\epsilon_{rr} = \frac{du}{dr} \quad \epsilon_{\varphi\varphi} = \frac{u}{r} \\ \epsilon_{zz} = \frac{dv}{dz} \quad \epsilon_{rz} = \frac{du}{dz} + \frac{dv}{dr} \tag{6}$$

where, radial and axial displacement component is u and v, respectively. The final displacement components equations are obtained by substituting Eqs. (5) and (6) into (3) and (4), and the two equations are resolved iteratively by the FVM.

VMS is represented as σ_{von} to calculate the level of thermal stress components,

$$\sigma_{von} = \left(\frac{3}{2}S_{ij}S_{ij}\right)^{1/2} \tag{7}$$

where S_{ij} is the stress deviator,

$$S_{ij} = \sigma_{ij} - \frac{1}{3}\sigma_{kk}\delta_{ij} \tag{8}$$

δ_{ij} Kronecker Delta

Normal strain and shear strain cause change in volume and shape which leads to top distortion.

Using stress components, we can calculate the von Mises stress, From Distortional (von Mises) energy theory

Distortion Strain Energy = Total Strain Energy – Volumetric strain Energy

$$\boldsymbol{\sigma}_{vonMises} = \frac{\sqrt{(\boldsymbol{\sigma}_1 - \boldsymbol{\sigma}_2)^2 + (\boldsymbol{\sigma}_2 - \boldsymbol{\sigma}_3)^2 + (\boldsymbol{\sigma}_3 - \boldsymbol{\sigma}_1)^2}}{2}$$

$$\sigma_{ex} = \begin{cases} 0 & \sigma_{von} \le \sigma_{crss} \\ \sigma_{von} - \sigma_{crss} & \sigma_{von} > \sigma_{crss} \end{cases}$$

σ_{ex} Excessive stress

σ_{crss} Critically resolved shear stress

The excessive stress (σ_{ex}) generates the dislocation during the growth process.

Calculate the vertical component of the growthvelocity

$$V_{crys} = \frac{1}{|n_x|\rho_{crys}\Delta H}(\lambda_{crys}\frac{\partial T_{crys}}{\partial n} - \lambda_{melt}\frac{\partial T_{melt}}{\partial n} \\ + (\varrho_{rad}^{in} - \varrho_{rad}^{out})crys - (\varrho_{rad}^{in} - \varrho_{rad}^{out})melt$$

where, V_{crys} is the crystallization rate, n is the normal to the surface, n_x is the cosine of the angle, ρ_{crys} is the crystal density, ΔH is the latent heat, λ_{crys} and λ_{melt} are the thermal conductivities in the crystal and melt respectively, $\frac{\partial T_{crys}}{\partial n}$ and $\frac{\partial T_{melt}}{\partial n}$ are the normal derivatives at the interface in the crystal and melt.

4 Results and Discussion

4.1 Axial Temperature Distribution

The growth rate of the growing ingot mainly depends on the axial temperature gradient [27]. If there is higher axial temperature gradient there will be higher growth rate and if there is lower axial temperature gradient there will be lower growth rate. Higher axial temperature gradient results in faster solidification and it induces the thermal stress during the growth process of ingot which can enhance the dislocations generation and multiplication. Using numerical simulation, the axial temperature gradient of the mc-Si ingot at the end of the solidification process was studied for various HEB thickness (50–250 mm) DS furnaces. The simulations have been performed for those furnace with the same input parameters. The simulation results of various HEB thickness in the DS furnace showed that the increase of HEB thickness results in the decrease of axial temperature gradient. The higher amount of heat is maintained inside the crucible when the insulation is high (250 mm). Since the temperature of the melt-crystal interface is fixed at 1685 K, the lower axial temperature gradient in the crystal region is maintained when the HEB thickness is high (250 mm). Figure 2 shows the plot of axial temperature with ingot height at the centre.

4.2 Radial Temperature Distribution

Control of radial temperature difference is very challenging. Here we have studied the radial temperature distribution using the numerical simulation. The radial temperature distribution reveals the shape of the melt-crystal interface. The radial temperature gradient of the ingot is influenced by the thermal behavior of the quartz crucible. The temperature distribution at the bottom of the ingot from the center to peripheral region is shown in Fig. 3. As we discussed in the earlier section the HEB with higher thickness is maintained at higher temperature due to massive storage of heat. The crucible bottom is maintained at higher temperature due to the higher thickness and

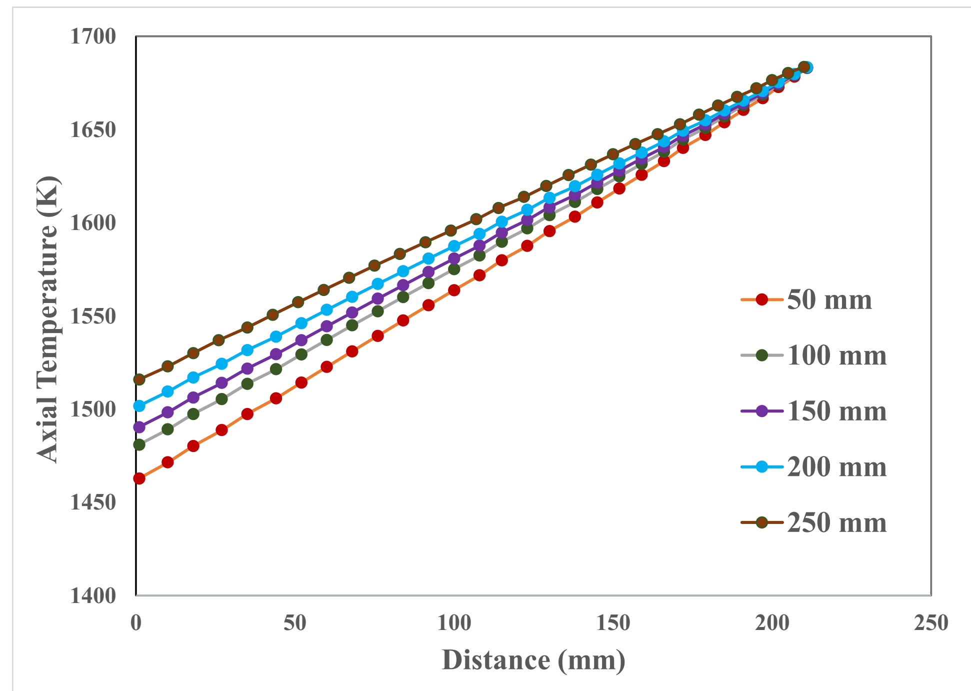

Fig. 2 The axial temperature of the multi-crystalline silicon ingot at the end of the DS for various HEB

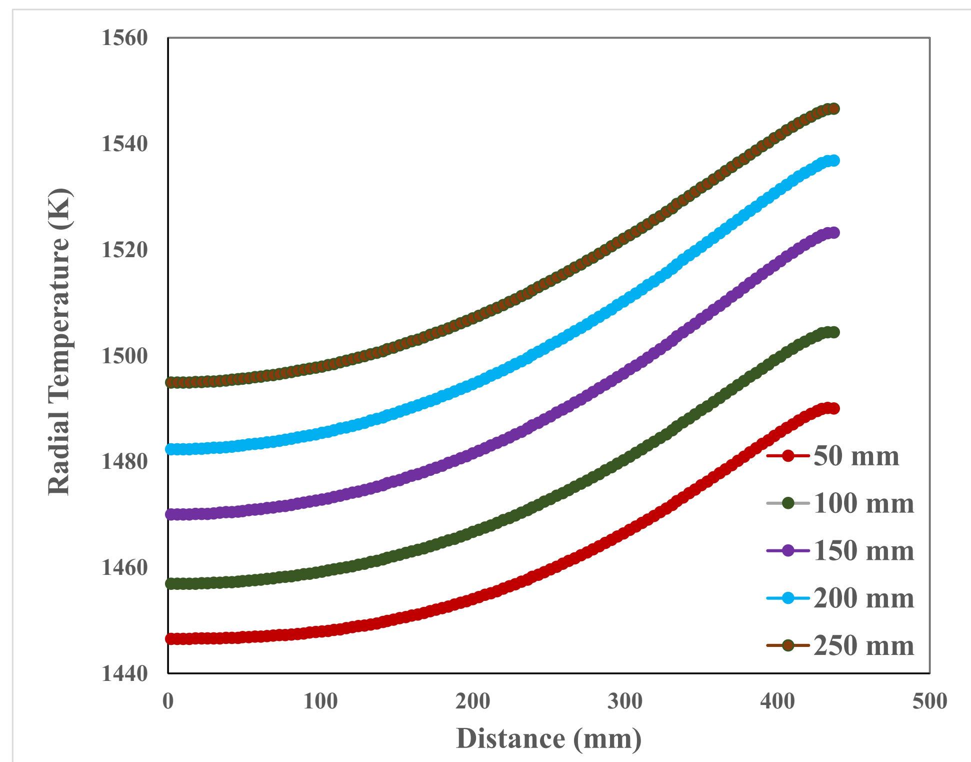

Fig. 3 The bottom radial temperature distribution of ingot at the end of the DS for various HEB

the bottom radial temperature distribution is decreased by decreasing the thickness of the insulation block. The generation of VMS is due to the combination of axial and radial temperature distribution.

4.3 Growth Rate

Growth rate is one of the important factors which could affect the multi-crystalline silicon ingot quality during the solidification process. The temperature, cooling rate and heat exchanger

block play a vital role in the growth of the crystal. By changing the temperature gradient, growth rate could be controlled which can be established by desirable thickness of the HEB. The DS process is a simpler process which can be used to produce larger size mc-Si ingots. Lower growth rate could suppress the development of dislocations produced by thermal stress and also decrease the efficiency. The production efficiency is increased though larger crystal growth rate but it decreases the quality by introducing defects. To improve production efficiency, it is better to start with lower growth rate at initial stage and higher growth rate at later stage. The variation in the rate of crystal growth for different HEB is plotted in Fig. 4. In all those cases the higher initial growth rate was observed which is due to the faster lifting of the side insulation to start the nucleations at the crucible bottom. The density of the solid silicon is lower than liquid silicon and it may lead to floating of solid silicon if we start the crystal growth with lower growth rate, so there is a need to form the bulk crystal at the bottom of the crucible. The proper heat transfer is established in the growth region depending on thickness of the HEB. The thicker HEB releases lower heat in the growth region which results in the lower growth rate. Since the growth rate is depending on the axial temperature gradient which can be varied by the thickness of the HEB, the growth rate is directly controlled by the HEB thickness. The results showed that the increase of HEB thickness causes decrease in growth rate. The lower growth rate was obtained at 250 mm HEB thickness and higher growth rate was observed at 50 mm thickness HEB. The growth rate is increasing linearly when the HEB thickness decreases from 250 to 50 mm, so that the higher growth rate can be established while using 50 mm thickness HEB and lower growth rate can be established while using 250 mm thick HEB. From 15 to 25th hour the growth rate for all those cases is maintained around 6 mm/hr to achieve controlled annealing or cooling process in which it will reduce temperature gradient along axial and radial direction within the ingot there by reducing the defects and dislocations within the grown ingot. Outgoing heat flux is controlled by HEB. Even though the growth rate depends on the heater power and opening rate of insulation, the thickness of heat exchanger block is purposely increased to achieve controlled growth of ingot where the heat dissipation at the bottom is controlled by increasing the insulation thickness. So, by optimizing the thickness of the insulation block, we can control the temperature gradient along the radial and axial direction of the growing ingot. Here the variation in the growth rate is due to the variation in heater power reduction rate. The larger variations in growth rate will affect the crystal quality. The variation in growth rate is rather low in our case which will not affect the crystal quality. In this period if the equilibrium heat transfer is attained then the insulation is further lifted to enhance the heat transfer.

4.4 Maximum Principal Stress

The maximum principal stress is determined by HEB thickness. In the DS method, the maximum principal stress in the multi-crystalline silicon ingot is the key factor to identify ingot quality. Hydrostatic Stress which is derived from the

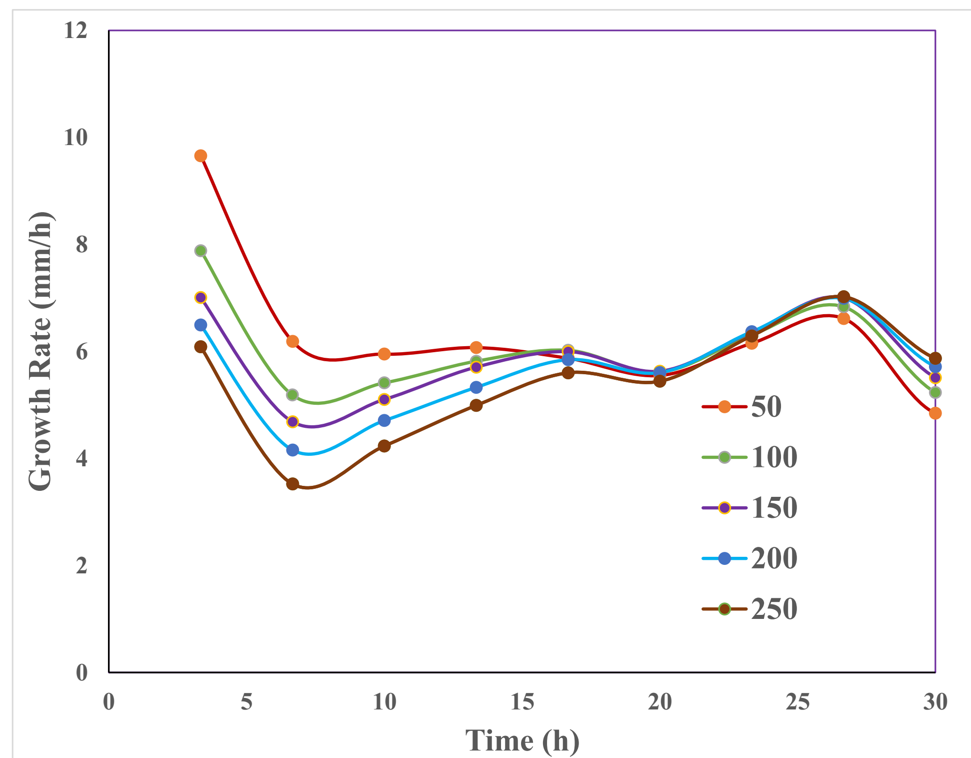

Fig. 4 Growth rate for various thickness of HEB

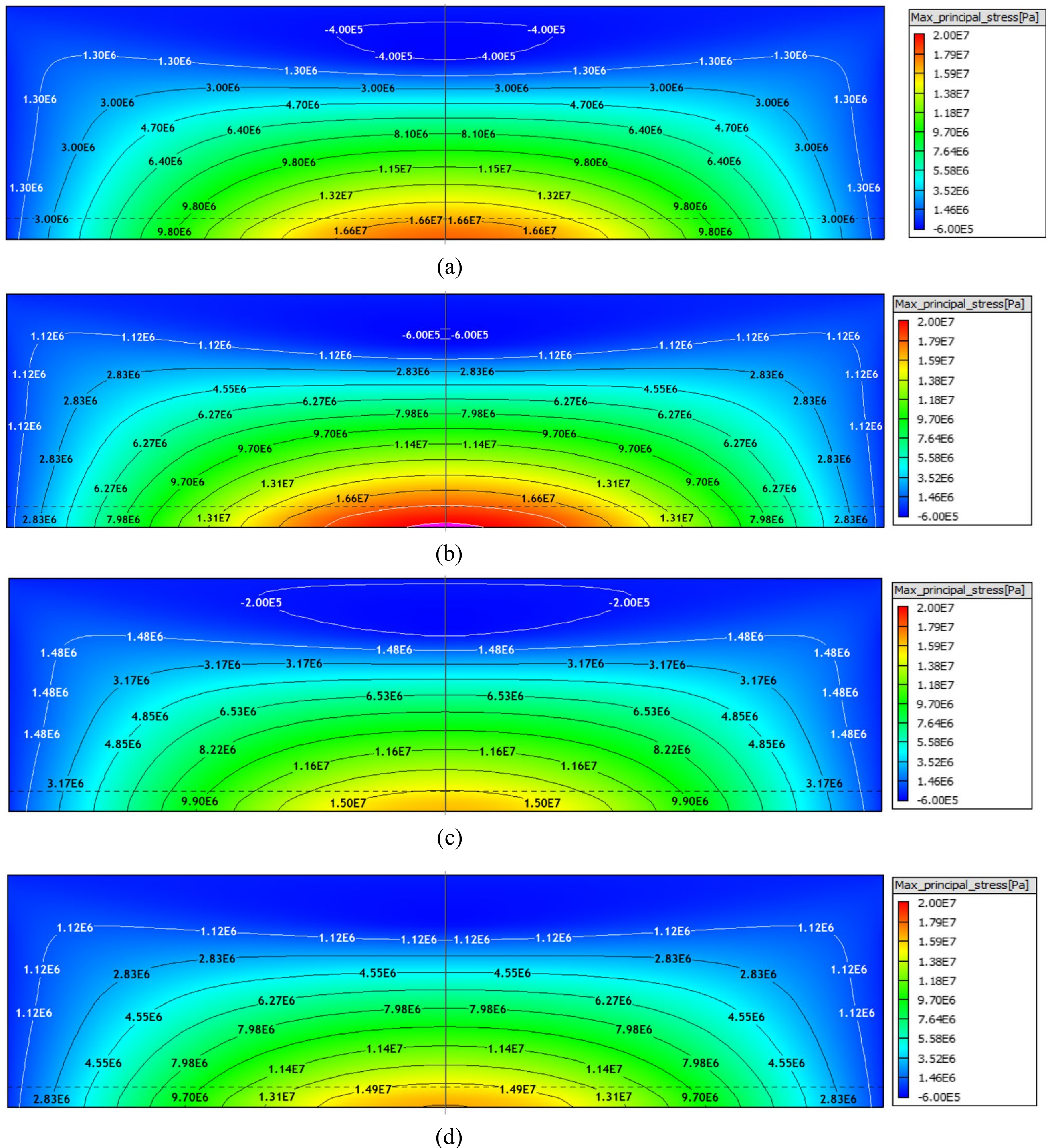

Fig. 5 Maximum principal stress (MPa) of mc-Si ingot for various thickness of HEB. **a**, **b**, **c** and **d** corresponding to the 100 mm, 150 mm, 200 mm and 250 mm HEB thickness

stress tensors will lead to VMS and some of the components of the maximum principal stress tensor lead to the development of the VMS in the multi-crystalline silicon ingot. The simulations are done for various thickness of HEB and the results are compared. The distribution of maximum principal stress in the multi-crystalline silicon ingot is: 100 mm > 150 mm > 200 mm > 250 mm. It is shown in Fig. 5. The heat extraction decreases with increase in heat exchanger block thickness and this results in decrease in maximum principal stress as thickness of heat exchanger block increases. 250 mm thickness will be the better choice for the growth. In the bottom, the stress is decreasing as HEB thickness increases.

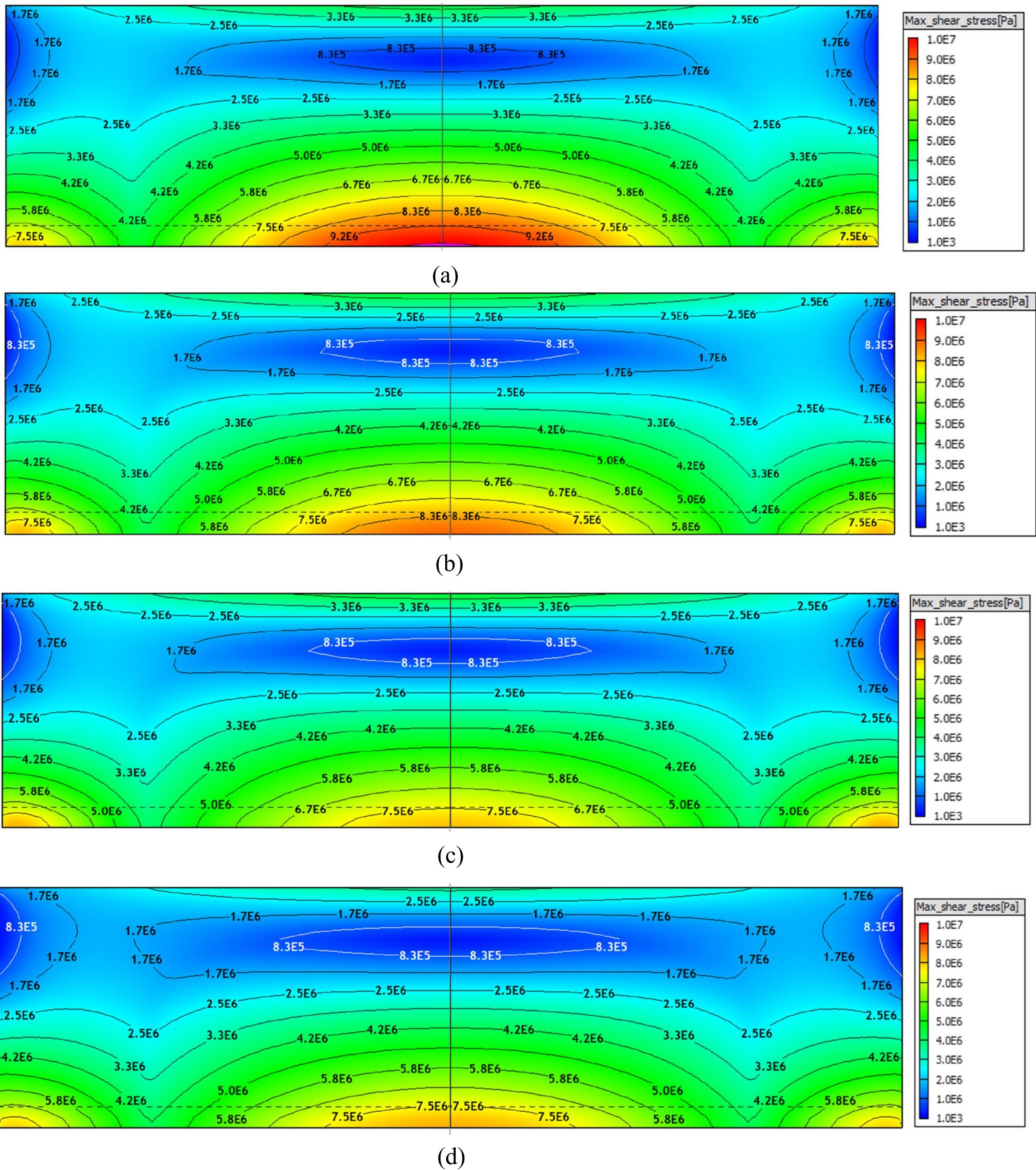

Fig. 6 Maximum shear stress (MPa of mc-Si ingot for various thickness of HEB. **a**, **b**, **c** and **d** corresponding to the 100 mm, 150 mm, 200 mm and 250 mm HEB thickness

4.5 Maximum Shear Stress

Shear stress is caused by non-homogeneous temperature. To avoid the shear stress, optimization of the temperature gradient during the solidification is important. The distribution order of maximum shear stress in the multi-crystalline silicon ingot is as follows: 100 mm > 150 mm > 200 mm > 250 mm. It is shown in Fig. 6. Results

show that the shearing stress decreases with increase in thickness of the heat exchanger block. The heat extraction decreases with increase in heat exchanger block thickness and this results in decrease in shear stress as thickness of heat exchanger block increases. The components of stress tensor is important since it plays main role to determine the VMS distribution and dislocation formation. The growth rate for all those cases was not increased more than 10 mm/hr and those have given lower VMS, the distributions of maximum shear stress in the mc-Si ingot are also in optimal range. In the bottom, the maximum shear stress is decreasing as HEB thickness increases. The heat extraction decreases with increase in heat exchanger block thickness and this results in decrease in maximum shear stress as thickness of heat exchanger block increases. So, 250 mm thickness will be the better choice for the growth of improved ingot quality.

4.6 Von-Mises Stress

The distortion in the crystal is change in the volume and shape due to the normal strain and shear. Using stress components we can calculate the von Mises stress, from distortional (von Mises) energy theory. The allowed critical stress value for CZ grown crystal is about 30–35 Mpa. But in mc-Si there is no such explicit limitation due to the presence of grain boundaries. Rao et al. [28] also reported that narrow bottom insulation is beneficial for the reduction of the thermal stress.

The VMS is used to predict the yielding of materials under complex loading condition. Normally if there is equal loading on each side of the material it will cause the change in volume which will not induce the VMS in the material. The distribution order of von Mises stress in the multi-crystalline silicon ingot is as follows: 100 mm > 150 mm > 200 mm > 250 mm. It is shown in Fig. 7. In our case five sides of the growing ingot are surrounded by the rigid crucible walls and the top surface of the crucible is free for expanding. On the time of solidification process the growing ingot feels stress from five sides of crucible wall due to the thermal expansion and the top surface of the ingot will expand freely. Due to this complex loading condition the VMS will be induced in the growing ingot. Hence the generation and multiplication of dislocations will start. Hence, the lower axial temperature gradient with higher radial temperature gradient and the higher axial temperature gradient with lower radial temperature gradient induce the increase in VMS in the growing multi-crystalline silicon ingot. Here, lower VMS in all the cases is due to the lower growth rate (< 10 mm/hr). The recommended growth rate is 10 mm/hr. The controlled solidification can be obtained when the growth rate is around 10 mm/hr [27]. The von Mises stress increases with increase in thickness of the heat exchanger block and this is due to increase in radial temperature gradient within the growing ingot. The higher thickness increases the heat retention and increases the radial temperature during the growth there by causing defects and dislocation within the growing ingot. And so, the higher thickness of heat exchanger block is suitable for growing high quality crystals and the lower thickness such as above 200 mm is appropriate to quality ingot and higher thickness of heat exchanger block is not preferred. The higher VMS has been observed at the bottom and top region of the mc-Si ingot. The good quality with lower stress region has been obtained in the middle region of the mc-Si ingot. During the brick making process the higher VMS regions are trimmed in order to make high efficiency solar cells.

5 Conclusion

Numerical simulation has been carried out for DS system with various thickness of HEB. Axial temperature distribution and radial temperature distribution were analyzed by varying the thickness of the HEB in DS furnace. The influence of HEB in the DS furnace on the growth rate was analyzed. Moreover, the Maximum principal stress, shear stress and VMS distribution in the mc-Si ingot for various thickness of HEB have been analyzed. From the stress analysis 250 mm simulated results have lower principal stress, shear stress and von Mises stress than other cases. From this investigation 250 mm heat exchanger block may help to increase the mc-Si ingot quality for PV application.

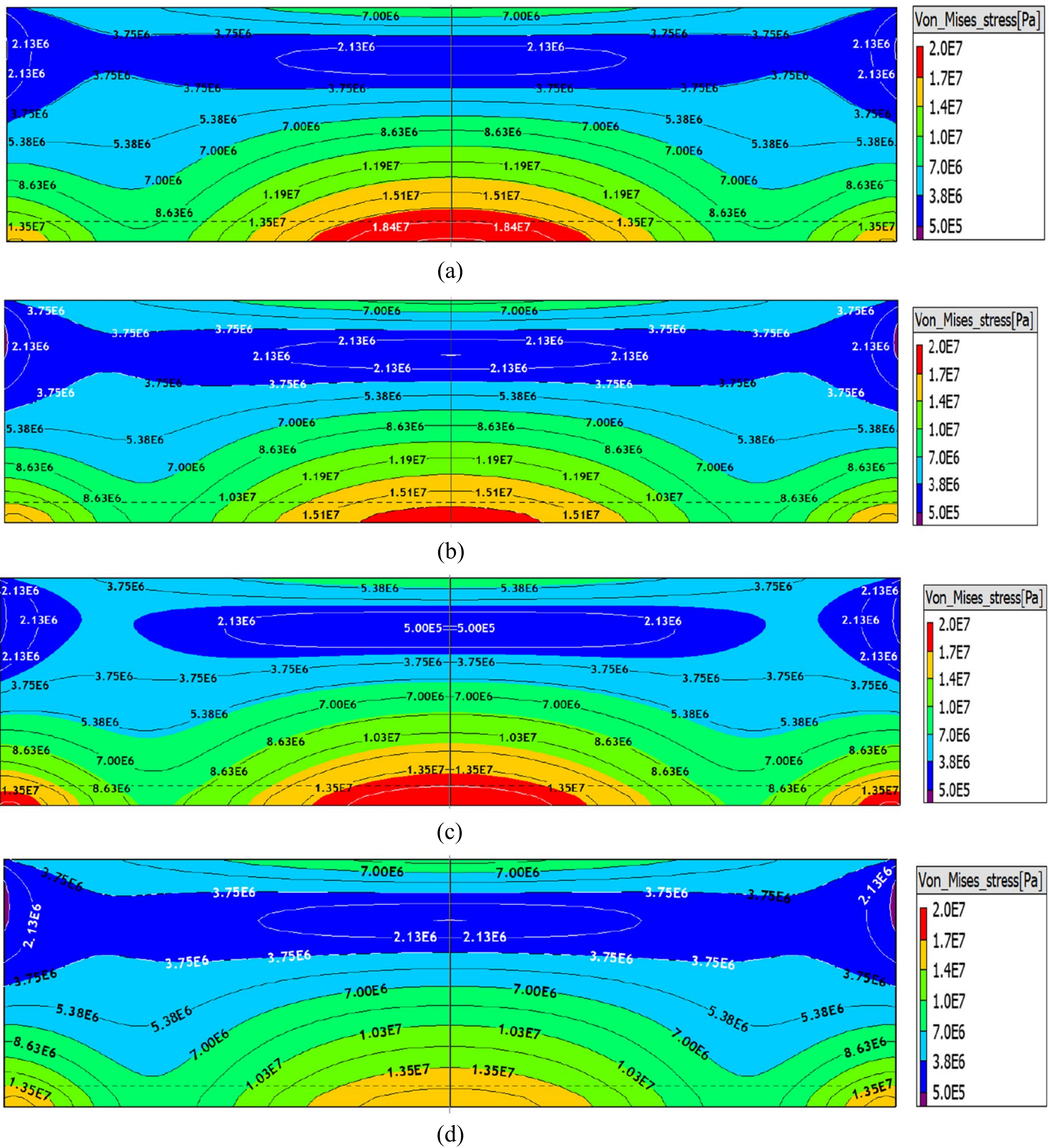

Fig. 7 Maximum von Mises stress (VMS) of mc-Si ingot for various thickness of HEB. **a**, **b**, **c** and **d** corresponding to the 100 mm, 150 mm, 200 mm and 250 mm HEB thickness

Acknowledgments This work was supported by the Ministry of New and Renewable Energy (MNRE), the Government of India (Order no: 31/58/2013-2014/PVSE & 15-01-2015). G Aravindan acknowledges Human Resource Development Group, Council of Scientific & Industrial Research (CSIR) for Senior Research Fellowship, Government of India (Sanction letter no/file no: 08/542(0010)2K19 EMR-I).

Authors' Contributions

Authors	*Contribution*
Anbu Gopalakrishnan	*Software, Conceptualization, Formal analysis, Investigation, Data Curation, Writing—Original Draft, Writing—Review & Editing*
Thiyagarajan Madhu	*Software, Validation, Formal analysis, Investigation*
Aravindan Gurusamy	*Software, Validation, Formal analysis, Investigation*
Srinivasan Manikkam	*Supervision*
Ramasamy Perumalsamy	*Software, Validation, Formal analysis, Investigation*

Data Availability Not applicable.

Code Availability CGSim – a commercial software was used.

Declarations

Ethics Approval Not applicable.

Consent to Participate Not Applicable.

Consent for Publication Not Applicable.

Conflicts of Interest/Competing Interests The authors have no conflicts of interest to declare that are relevant to the content of this article.

References

1. Nguyen THT, Chen JC, Hu C, Chen CH, Huang YH, Lin HW, Yu A, Hsu B (2017) Numerical analysis of thermal stress and dislocation density distributions in large size multi-crystalline silicon ingots during the seeded growth process. J Cryst Growth 468:316–320
2. Aldous JD, Burrows CW, Maskery I, Brewer M, Pickup D, Walker M, Mudd J, Hase TP, Duffy JA, Wilkins S, Sanchez-Hanke C (2012) Growth and characterisation of NiSb (0001)/GaAs (111) B epitaxial films. J Cryst Growth 357:1–8
3. Chen W, Wu Z, Zhong G, Ding J, Yu Y, Zhou X, Huang X (2016) Optimization of heat transfer by adjusting power ratios between top and side heaters for casting high-performance multi-crystalline silicon ingots. J Cryst Growth 451:155–160
4. Keerthivasan T, Chen CJ, Sugunraj S, Srinivasan M, Ramasamy P (2022) Influence of Radiation Heat Transfer on Mc-Si Ingot during Directional Solidification: A Numerical Investigation. Silicon 1–10
5. Nagarajan SG, Sanmugavel S, Kesavan V, Aravindan G, Srinivasan M, Ramasamy P (2019) Influence of additional insulation block on multi-crystalline silicon ingot growth process for PV applications. J Cryst Growth 516:10–16
6. Kumar MA, Aravindan G, Srinivasan M, Ramasamy P, Kakimoto K (2022) Numerical Analysis of Melt Flow and Interface Deflection during the Growth of Directional Solidified Multi-Crystalline Silicon Ingots of Three Different Dimension. SILICON 14(6):3049–3057
7. Su W, Li J, Yang W, Han X, Guan Z, Zhang Z (2022) Numerical Investigation of Bottom Grille for Improving Large-Size Silicon Quality in Directional Solidification Process. SILICON 14(1):211–221
8. Gurusamy A, Manickam S, Perumalsamy R (2022) Quality improvement of multi-crystalline silicon ingot by the Hot-Zone modification. J Cryst Growth 126720
9. Yoo KC, Johnson SM, Regnault WF (1985) Effect of Metal Impurities in Silicon Feedstock on Multi crystalline Silicon Solar Cells. J Appl Phys 157:2258
10 Jouini A, Ponthenier D, Lignier H, Enjalbert N, Marie B, Drevet B, Pihan E, Cayron C, Lafford T, Camel D (2012) Prog Photovolt Res Appl 20(6):735–746
11. Gao B, Nakano S, Harada H, Miyamura Y, Sekiguchi T, Kakimoto K (2015) Single-seed casting large-size monocrystalline silicon for high-efficiency and low-cost solar cells. Engineering 1(3):378–383
12. Chen XJ, Nakano S, Liu LJ, Kakimoto K (2008) Study on thermal stress in a silicon ingot during a unidirectional solidification process. J Cryst Growth 310:4330–4335
13. Chen XJ, Nakono S, Liu L, Kakimoto K (2008) Reports of research institute for applied mechanics, No. 135. Kyushu University, Japan 45–52
14. Wang S, Fang HS, Zhao CJ, Zhang Z, Zhang MJ, Xu JF (2015) Gas flow optimization during the cooling of multicrystalline silicon ingot. Int J Heat Mass Transf 84:370–375
15. Zhou N, Lin M, Zhou L, Hu Q, Fang H, Wang S (2013) A modified cooling process in directional solidification of multicrystalline silicon. J Cryst Growth 381:22–26
16. Gurusamy A, Manickam S, Karuppanan A, Perumalsamy R (2018) Simulation Studies of Annealing Effect on a mc-Si Ingot for Photovoltaic Application. SILICON 10(3):1021–1033
17. Ding C, Huang M, Zhong G, Ming L, Huang X (2014) A design of crucible susceptor for the seeds preservation during a seeded directional solidification process. J Cryst Growth 387:73–80
18. Wu Z, Zhong G, Zhang Z, Zhou X, Wang Z, Huang X (2015) Optimization of the high-performance multi-crystalline silicon solidification process by insulation partition design using transient global simulations. J Cryst Growth 426:110–116
19. Ma W, Zhong G, Sun L, Yu Q, Huang X, Liu L (2012) Influence of an insulation partition on a seeded directional solidification process for quasi-single crystalline silicon ingot for high-efficiency solar cells. Sol Energy Mater Sol Cells 100:231–238
20. Qiu S, Wen S, Fang M, Zhang L, Gan C, Jiang D, Tan Y, Li J, Luo X (2016) Process parameters influence on the growth rate during silicon purification by vacuum directional solidification. Vacuum 125:40–47
21. Vasiliev MG, Mamedov VM, Rukolaine SA, Yuferev VS (2009) Heat source optimization in a multisection heater for the growth of bismuth germanate crystals by the low-gradient Czochralski method. Bull Russ Acad Sci Phys 73(10):1406–1409
22. Ostrogorsky AG (2013) Combined-convection segregation coefficient and related Nusselt numbers. J Cryst Growth 380:43–50

23. Zhao W, Liu L, Sun L (2014) Quality evaluation of multi-crystalline silicon ingots produced in a directional solidification furnace with different theories. J Cryst Growth 401:296–301
24. Wu Z, Zhong G, Zhou X, Zhang Z, Wang Z, Chen W, Huang X (2016) Upgrade of the hot zone for large-size high-performance multi-crystalline silicon ingot casting. J Cryst Growth 441:58–63
25. Nakano S, Chen XJ, Gao B, Kakimoto K (2011) Numerical analysis of cooling rate dependence on dislocation density in multicrystalline silicon for solar cells. J Cryst Growth 318(1):280–282
26. Nagarajan SG, Srinivasan M, Aravinth K, Ramasamy P (2019) Improving heat transfer properties of DS furnace by the geometrical modifications for enhancing the multi crystalline silicon ingot (mc-Si) quality using transient simulation. Silicon, 11(2):603–613
27. Rao S, Chen XH, Zhang F, He L, Luo Y, Xiong H, Hu Y, Wang F, Song B (2020) Influence of modified bottom insulation on the seeded directional solidification process for high-performance multi-crystalline silicon. Vacuum 172:108969
28. Lan CW, Yang CF, Lan A, Yang M, Yu A, Hsu HP, Hsu B, Hsu C (2016) Engineering silicon crystals for photovoltaics. CrystEngComm 18(9):1474–1485

Publisher's Note Springer Nature remains neutral with regard to jurisdictional claims in published maps and institutional affiliations.

Springer Nature or its licensor holds exclusive rights to this article under a publishing agreement with the author(s) or other rightsholder(s); author self-archiving of the accepted manuscript version of this article is solely governed by the terms of such publishing agreement and applicable law.